Rationale for Shallow Foundation Rocking Provisions in ASCE 41-13

Bruce L. Kutter,[a] **M.EERI, Mark Moore,**[b] **M.EERI,**
Manouchehr Hakhamaneshi,[a] **M.EERI, and Casey Champion,**[b] **M.EERI**

ASCE 41-13 supports three methods of modeling the soil-structure interaction for rocking footings as components of a foundation-building system: Method 1 uses uncoupled moment, shear, and axial springs; Method 2 uses a nonlinear gapping bed of springs; and Method 3 is used for structural footings that are flexible relative to the underlying soil. New component action tables in ASCE 41-13 provide modeling parameters and acceptance criteria for nonlinear and linear analysis of shallow foundation components. The values in the component action tables for nonlinear procedures were largely based upon analysis of foundation performance in model tests on rocking foundations. The primary measure to assess foundation performance is residual settlement or uplift. The acceptance criteria for linear analysis procedures (*m*-factors) were derived from the allowable rotations for nonlinear procedures. A design example is presented in an online Appendix to illustrate differences between the current and previous versions of ASCE 41 and ASCE 31. [DOI: 10.1193/121914EQS215M]

INTRODUCTION TO ASCE 41-13

ASCE/SEI 41-13, *Seismic Evaluation and Retrofit of Existing Buildings*, is an update of ASCE 41-06 combined with some provisions from ASCE 31-03. This paper describes the rationale (analysis and tests results) used for the development of new provisions associated with rocking shallow foundations in ASCE/SEI 41-13 (henceforth simply referred to as ASCE 41). A companion paper (Hakhamaneshi et al. 2016) presents new independent test results obtained after the approval of ASCE 41-13; their new results largely validate and to some extent suggest refinement of the new provisions for rocking shallow foundations.

PERFORMANCE LEVELS AND ANALYSIS PROCEDURES

The standard implements performance-based design concepts by establishing a matrix of one or more *target building performance objectives* consisting of pairings of performance levels and earthquake hazard levels. Primary performance levels include immediate occupancy (IO), life safety (LS), and collapse prevention (CP). Hazard levels are referred to by their probability of exceedance in a specified time period and may include, for example,

[a] Dept. of Civil & Environ. Engrg., UC Davis. 1 Shields Ave, Davis, CA 95616. blkutter@ucdavis.edu, mhakhamaneshi@ucdavis.edu
[b] ZFA Structural Engineers, SE, LEED AP, markm@zfa.com, caseyc@zfa.com

Earthquake Spectra, Volume 32, No. 2, pages 1097–1119, May 2016;

a motion with a 2% probability of exceedance in 50 years and/or 50% probability of exceedance in 50 years.

ASCE 41 allows four types of analysis procedures for evaluation of performance: linear static procedure (LSP), linear dynamic procedure (LDP), nonlinear static procedure (NSP) and nonlinear dynamic procedure (NDP).

In the nonlinear procedures, the entire building is modeled as a nonlinear system; the nonlinear components of the system (e.g., beams, columns, connections, and foundations) are represented using modeling parameters listed in the nonlinear component action tables provided in ASCE 41, which also provide acceptance limits for the demand placed on each component. For the LSP and LDP, the linear analysis is expected to produce displacements that approximate maximum displacements expected for the selected hazard, but will produce internal forces that exceed those that would be obtained in a yielding building. The acceptance criteria include modification factors (*m*-factors) to account for anticipated inelastic response demands and capacities.

Linear Static Procedure (LSP)

The LSP involves determination of the natural period of a building and estimation of the pseudo-seismic force based upon the design response spectrum with modifications to account for expected ductility and the shape of hysteresis curves for the materials used in the building. The calculated force is also modified to account for higher modal mass participation effects. The standard provides equations for how the pseudo-seismic forces are to be distributed over the height of the building in order to determine the elastic demands on individual components of the building system.

According to Poland (2008), the linear static procedure (LSP) is the first and simplest level of analysis; it provides an equivalent lateral force, vertical distribution of forces and rules for modeling, and acceptance criteria. It is similar to the lateral force procedure from the codes of the 1970s and 1980s, except that the base shear is much higher and the ductility factors (or *m*-factors) are much smaller. "It is intended to be simple and very conservative to allow one and two story buildings of regular configuration to pass because of their excessive strength." Poland (2008, p. 16) further states: "The LSP should only be used to show that a building is okay, not to determine the extent of strengthening it might need."

Linear Dynamic Procedure (LDP)

For the linear dynamic procedure, input motion is specified on the boundaries of a numerical model of the building and time history analysis is conducted to determine the maximum force demands on a linear elastic system, modeled using the effective stiffness for member actions. Alternatively, seismic loads may be characterized by a modal response spectrum analysis. For the LDP, the standard permits foundations to be modeled as rigid (fixed-base) or flexible.

Nonlinear Static Procedure (NSP)

For the nonlinear static procedure, the shape of the force distribution is assumed to be constant for any one load case (varying vertical distribution profiles, multiple load cases are recommended to bracket the solution), and the resultant input force is varied to predict a

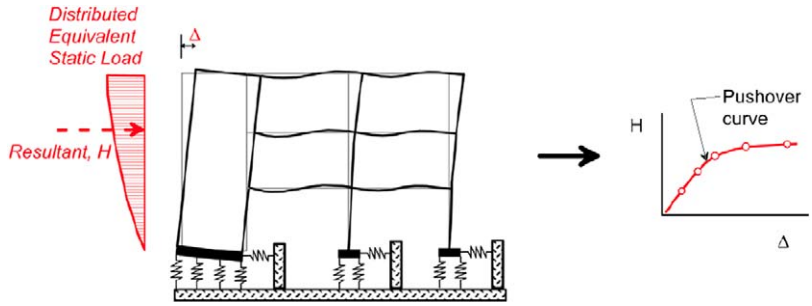

Figure 1. Example pushover analysis for Nonlinear Static Procedures (NIST 2012).

pushover (capacity) curve, as illustrated in Figure 1, to show the relation between the seismic load and expected displacement. The amplitude of the displacement demand may be estimated from the linear elastic deformation response spectrum $S_d(T_e, \beta)$ where T_e is the effective period (corresponding to the system secant stiffness at about 60% of the pushover yield strength) and β is the damping ratio (usually 5% but with exceptions depending on type of construction). While the global deformation of the building is determined by the spectrum analysis methods, the response of individual components (including the footings) is determined by a nonlinear static pushover analysis wherein the modeling parameters (stiffness, capacity and backbone curve) of each component may be determined in accordance with ASCE 41. Further details of this procedure are described in Chapter 7 of ASCE 41.

Nonlinear Dynamic Procedure (NDP)

The NDP involves calculation of the response history of a nonlinear building system to selected input ground motions. This method of analysis accounts for stiffness and hysteretic energy dissipation in each component of the building. Radiation damping associated with soil-structure interaction may also be accounted for by adding radiation dashpots to the linear components of the springs connecting the foundation to the input motion.

Component Action Tables

One feature of ASCE 41 is the inclusion of tables describing "Modeling Parameters and Acceptance Criteria" for modeling and evaluating many building components using linear and nonlinear procedures. In the concrete chapter, for example, there is a table describing the development of a backbone hysteresis curve for a plastic hinge in a reinforced concrete shear wall as a series of linear segments on a Moment-Rotation curve. The component action table for nonlinear analysis conveys how to model the backbone curve as well as the maximum rotation allowed for IO, LS, and CP performance levels. The linear tables in ASCE 41 provide acceptance criteria in terms of allowable *m*-factors for the linear static and dynamic analysis procedures.

MAJOR REVISIONS OF ROCKING FOUNDATION PROVISIONS

ASCE 41 supports three methods of modeling rocking footings as components of a foundation-building system. The methods, described in Figure 2, are Method 1 (uncoupled

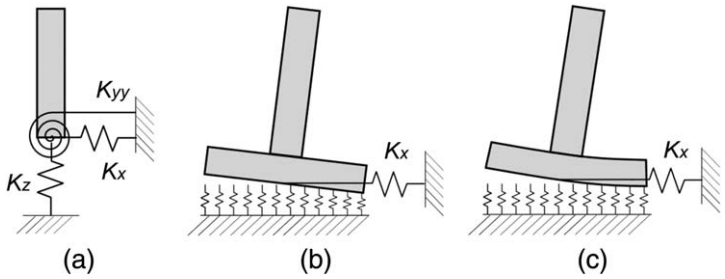

Figure 2. Methods for modeling rocking foundations in ASCE 41-13. (a) Method 1 using uncoupled springs, (b) Method 2 using nonlinear sub-grade reaction springs, and (c) Method 3 for cases where, the footing is flexible compared to the soil.

spring method), Method 2 (nonlinear gapping bed of springs), and Method 3 (for structural footings that are flexible compared to the soil). A new feature of ASCE 41 is the inclusion of component action tables for nonlinear and linear analysis of shallow foundation components. The numbers in the tables are largely based upon analysis of experimental data from tests on rocking foundations in geotechnical centrifuge and large scale tests. Using the nonlinear tables, acceptance criteria for linear procedures (*m*-factors) were derived.

Reasons for including the foundation rocking action modeling parameters and acceptance criteria, like any other structural component action, were to replace provisions that were outdated and to require a more explicit assessment of the foundation deformation effects on the structure. Another motivation for changes to the foundation provisions included the unrealistic definition for elastic soil springs with uncapped strength and assumed infinite soil ductility in ASCE 41-06, without considering the potential consequences of rocking, such as permanent foundation settlement. The core goal of the changes was to increase the accuracy of the building models, thereby structural component action assessment, by generally requiring inclusion and assessment of the soil-foundation interface effects. Further, the revisions provide acceptance criteria that aim to achieve the target performance objectives by controlling the displacement incompatibility associated with foundation settlement caused by rocking.

It is important to note that other sources of vertical displacement incompatibility (besides settlement) are present and are outside the scope of this particular standard update effort. For example, rotation of a shear wall and uplift due to rotation of a footing will cause vertical displacements of connections between the structure and the shear wall. While the acceptance criteria in the rocking provisions (in Chapter 8 of ASCE 41-13) are intended to limit permanent settlements of the footings, the acceptance criteria do not account for effects of cyclic vertical displacement incompatibility on the connections.

DESCRIPTION OF ROCKING SHALLOW FOUNDATIONS

Shallow footings envisioned in ASCE 41 have a flat (or stepped) base with the ratio of embedment depth, D_f, to length of the foundation, L, less than 1. Shallow foundations may be designed to rock using the new ASCE 41 provisions if they are supported on competent

ground that does not suffer significant strength loss due to earthquake shaking. The experimental data upon which the provisions are based did not include submerged footings. The procedures in ASCE 41 therefore do not account for the possibility of water pumping into the gap associated with uplift for high water table conditions. Gapping associated with uplift occurs when the moment about the base of the footing is sufficient to cause the structural footing to lose contact with the soil under the footing. A critical contact area along one edge of the footing will dig into the soil below while the other edge of the footing separates from the soil creating a gap between the footing and the soil. A local bearing failure will occur under the loaded edge as depicted in Figure 3. The critical contact area (A_c) is determined by the bearing capacity of the soil: $A_c = P/q_c$, where q_c is the expected soil bearing capacity corresponding to the loaded area, A_c.

ROCKING VS. SLIDING

The general approach in ASCE 41 allows for separate consideration of rocking, sliding and settlement deformations. However, the new component action tables in the standard assume that rocking is the dominant source of deformation. Additional work is required to develop component action tables for footing sliding or coupled rocking and sliding (Hakhamaneshi 2014). ASCE 41 provides general modeling procedures for sliding foundation actions but limited guidance on acceptance criteria. Rocking with footing uplift is considered to be preferred over sliding because gapping produces a natural recentering mechanism associated with closure of the gap upon unloading. Floor slabs and grade beams might be of significant benefit in restraining sliding while allowing rocking.

METHOD 1: UNCOUPLED MOMENT, SHEAR, AND AXIAL SPRINGS

ASCE 41 allows three different methods for analyzing rocking foundations, as depicted in Figure 2. Method 1 involves the use of uncoupled moment, shear and axial springs (moment and shear behavior is independent of the axial load on the footing). If there is significant variation in axial load, P, due to frame action, Method 2 is preferable over Method 1 because Method 2 explicitly accounts for the coupling between rotation and vertical deformation.

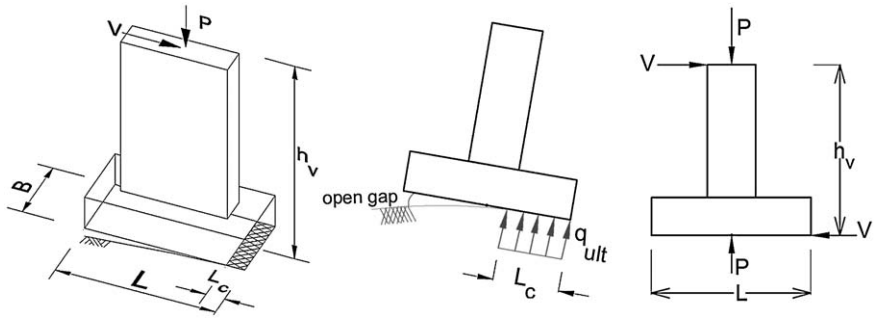

Figure 3. Footing shape parameters for rectangular and I-shaped rocking footings.

MODELING PROCEDURES FOR UNCOUPLED NONLINEAR SPRINGS

Method 1 is for rocking foundations with relatively rigid structural footings, analyzed using uncoupled springs that connect the base of the structural member to the ground. For nonlinear analysis, ASCE 41 recommends that the initial stiffness of the springs (along AF in Figure 4) is to be determined using the conventional elastic solutions contained in the standard. One bilinear horizontal and one bilinear vertical spring define the lateral and axial translational stiffness and strength; the assumed bilinear load-deformation behavior is illustrated in Figure 4a. One trilinear rotational spring, illustrated in Figure 4b is used to represent the nonlinear moment-rotation behavior. The capacity of the shear and axial springs (Q_y) may be derived from conventional methods of foundation analysis. For rectangular or I-shaped foundations, the moment capacity, M_c, of the rotational spring is determined from Equation 1, and does not vary during seismic shaking.

$$M_c = \frac{PL}{2}(1 - \rho_{ac}) \tag{1}$$

where $\rho_{ac} = A_c/A$ is called the critical contact area ratio or compression ratio.

Note that the footing moment capacity is calculated about the centroid of the base of the soil-footing contact area. Defined this way, the moment capacity theoretically remains constant and does not diminish as the P-Δ moment increases. The applied moment in the analysis, therefore, must include the P-Δ moment.

For moment-rotation behavior, the component action table (Table 1) provides values for the modeling parameters d, f, and g (see Figure 4b) as a function of $\rho_{ac} = A_c/A$ and the aspect ratio b/L_c, where b is the footing width for rectangular footings and L_c is the length of the critical contact area. For I-shaped footings, b is defined as the minimum of the footing width or the "flange" width, t_f, and modeling parameters also depend on the "missing area ratio" $MAR = (A_{rectangle} - A)/A_{rectangle}$, graphically defined in Figure 5.

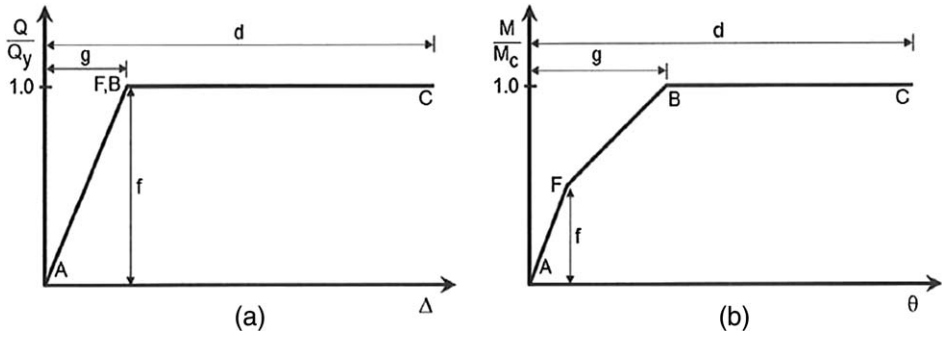

Figure 4. Load-deformation behavior for shallow foundations using Method 1 (uncoupled foundation springs) with a (a) bilinear relation for axial loading and shear loading, and (b) trilinear model for moment-rotation behavior.

Table 1. Centrifuge model and shake table tests used to determine modeling parameters

Reference	Test ID	Soil	L (m)	B (m)	D (m)	ρ_{ac}
G	SSG02_07	Sand, $D_r = 80\%$	2.8	0.65	0	0.384
G	SSG02_05	Sand, $D_r = 80\%$	2.8	0.65	0	0.384
G	KRR02_04	Sand, $D_r = 60\%$	2.7	0.65	0	0.294
G	SSG02_03	Sand, $D_r = 80\%$	2.8	0.65	0	0.192
G	SSG02_04	Sand, $D_r = 80\%$	2.8	0.65	0	0.137
G	SSG03_05	Sand, $D_r = 80\%$	2.8	0.65	0.65	0.142
G	SSG03_03	Sand, $D_r = 80\%$	2.8	0.65	0.65	0.071
G	SSG03_06	Sand, $D_r = 80\%$	2.8	0.65	0.65	0.050
G	SSG04_06	Sand, $D_r = 80\%$	2.8	0.65	0	0.323
G	KRR03_02	Clay, $S_u = 100$ kPa	2.7	0.65	0	0.357
D1	LJD01_LC	Sand, $D_r = 73\%$	12.2	7.79	2.24	0.0229
D1	LJD01_SC-2	Sand, $D_r = 44\%$	6.7	4.28	2.24	0.111
D2	LJD01_SC-1	Sand, $D_r = 73\%$	6.7	4.28	2.24	0.111
N	TRISEE_HD	Sand, $D_r = 85\%$	1	1	1	0.2
N	TRISEE_LD	Sand, $D_r = 45\%$	1	1	1	0.2
M	MAH01_SC_Al_1	Clay, $S_u = 60$ kPa	5.28	3.21	0	0.238
M	MAH01_SC_Al_1	Clay, $S_u = 70$ kPa	10.56	6.42	0	0.400
M	MAH01_SC_St_1	Clay, $S_u = 60$ kPa	6.66	6.66	0	0.500
K1	KRR02_S27-S32	Sand, $D_r = 60\%$	2.672	0.686	0	0.294
K1	KRR02_S41-S50	Sand, $D_r = 60\%$	2.672	0.686	0	0.294
K2	KRR03_S9-S17	Clay, $S_u = 100$ kPa	2.672	0.686	0	0.294
K2	KRR03_S18-S27	Clay, $S_u = 100$ kPa	2.672	0.686	0	0.294

References: G = Gajan and Kutter (2009), D1 = Deng et al. (2014), D2 = Deng and Kutter (2012), N = Negro et al. (2000), M = Hakhamaneshi et al. (2012), K1 = Rosebrook and Kutter (2001a), K2 = Rosebrook and Kutter (2001b).

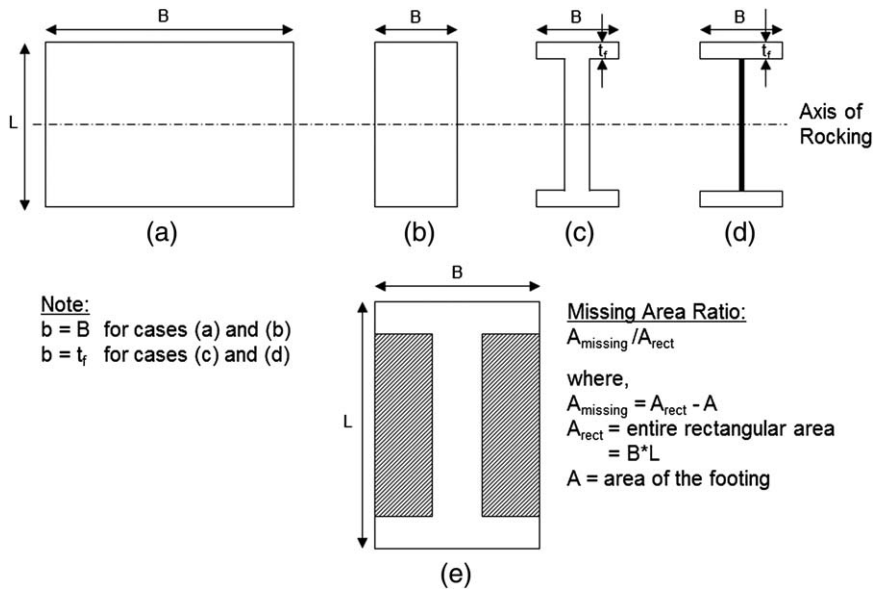

Figure 5. Characterization of footing shape.

For axial and shear behavior, as depicted in Figure 4a, a bilinear model is assumed for which the value of the parameter f is taken as 1. For flexural loading, the values of the parameters d, f, and g were obtained by analysis of a large amount of data from past experimental tests that are summarized in Table 2. To develop the values in Table 1, Johnson (2012) analyzed data from 14 researchers, including 16 tests on sand and 6 tests on clay, of

Table 2. Excerpts from Table 8-4 of ASCE 41-13: Modeling parameters and numerical acceptance criteria for nonlinear procedures

		Modeling parameters[1]				Acceptance criteria[1]		
						Total footing rotation angle, radians[2]		
Footing Shape			Footing rotation angle, radians		Elastic strength ratio	Performance level		
(a) Rectangle[3,4]								
b/L_c	$(A_{rect} - A)/A_{rect}$	A_c/A	g	d	f	IO	LS	CP
≥10	0	0.02	0.009	0.1	0.5	0.02	0.08	0.1
		0.13	0.013	0.1	0.5	0.015	0.08	0.1
		0.5	0.015	0.1	0.5	0.002	0.003	0.004
		1	0.015	0.1	0.5	0	0	0
3	0	0.02	0.009	0.1	0.5	0.02	0.068	0.085
		0.13	0.013	0.1	0.5	0.011	0.06	0.075
		0.5	0.015	0.1	0.5	0.002	0.003	0.004
		1	0.015	0.1	0.5	0	0	0
(b) I-shape[3,4]								
$1 \le b/L_c \le 10$	0.3	0.02	0.009	0.1	0.5	0.02	0.056	0.07
		0.13	0.013	0.1	0.5	0.007	0.04	0.05
		0.5	0.015	0.1	0.5	0.002	0.003	0.004
		1	0.015	0.1	0.5	0	0	0
$1 \le b/L_c \le 10$	0.6	0.02	0.007	0.1	0.5	0.015	0.048	0.06
		0.13	0.01	0.1	0.5	0.007	0.032	0.04
		0.5	0.011	0.1	0.5	0.0015	0.0023	0.003
		1	0.011	0.1	0.5	0	0	0

[1] Linear interpolation between values listed in the table shall be permitted.
[2] Allowable story drift >1%.
[3] Assumed rigid foundation modeled using uncoupled springs.
[4] Assumed rocking dominates over sliding: $(M/V)/L_f > 1$.

which 20 tests were performed on the centrifuge, and 2 tests on a shake table. Figure 6 shows how the trilinear model was fit to experimental results for moment-rotation hysteresis curves to obtain values of the parameters d, f, and g for each experiment.

All of the data analyzed were for footings with large moment to shear ratio ($M/VL > 1$), where M and V are the applied moment and shear load, respectively, and L is the footing length. In ASCE 41, the footing is considered to be rocking dominated if the normalized moment to shear ratio (M/VL) is greater than 1, and this restriction is stated in a footnote to the component action tables (Table 1). This lower limit on the normalized moment to shear ratio is based on the observations by Gajan and Kutter (2009) that the deformation at the loading point is predominantly caused by rotation, not sliding, if $M/VL > 1$; they also showed that the moment capacity is generally not reduced by more than about 20% due to the presence of the shear load if M/VL is greater than or equal to 1.

PARAMETER f

The moment capacity, M_c, of a rocking rigid block would be $M_c = PL/2$. The moment corresponding to a triangular distribution of pressure on the base of the footing is $PL/6$. The geometric nonlinearity (gapping) is expected to begin when the moment exceeds $PL/6$, at which point the elastic moment divided by the moment capacity would suggest $f \sim (PL/6)/(PL/2) = 1/3$. If the soil is not rigid, the moment capacity will be less than $PL/2$, and the value of f will, correspondingly, be greater than $1/3$. After exploring various possible values of f ($1/3$, $1/2$, and $2/3$), Johnson (2012) suggested that $f = 0.5$ is a good compromise and provides a good empirical fit to the data set summarized in Table 2.

PARAMETER g (ROTATION TO MOBILIZE MOMENT CAPACITY)

Once the parameter f was set to 0.5 as discussed above, and the moment capacity is obtained using Equation 1, the value of g was obtained for each experiment by visually adjusting g until the trilinear model best fit the experimental curve, as illustrated in Figure 6. Attention was made to make the total area under the curve to equal the total area under the

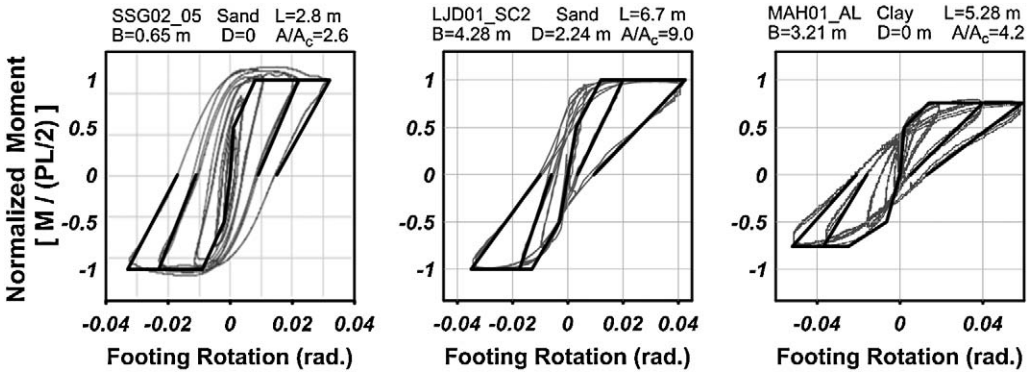

Figure 6. Rotation to mobilize capacity from ASCE 41-13 and experiments.

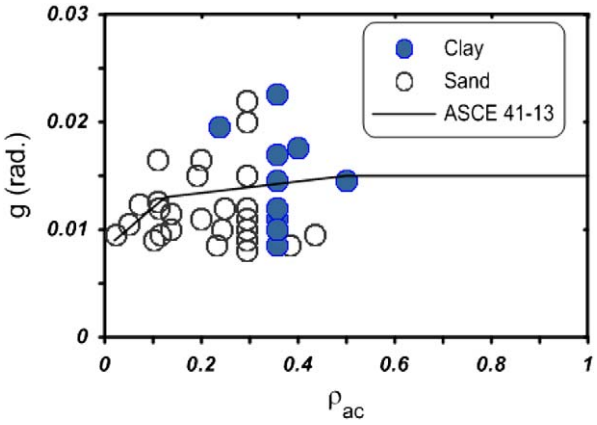

Figure 7. Observed relationship between footing rotation to mobilize moment capacity and the inverse of ρ_{ac} for rectangular footings in model tests.

trilinear relationship to preserve energy dissipation characteristics. The resulting values of the g parameter are summarized in Figure 7.

There is considerable scatter at large ρ_{ac}, but for values of ρ_{ac} less than 0.2, the values of g tend to lie in a limited range between 0.016 and 0.009 radians. The regression analysis by Johnson (2012) produced $g = 0.015$ for $\rho_{ac} = 0.5$, 0.013 for $\rho_{ac} = 0.13$, and 0.09 for $\rho_{ac} = 0.02$, and these three values were adopted as the recommended values for rectangular footings in Table 1.

PARAMETER *d* (MAXIMUM ROTATION)

To be consistent with other component action tables in ASCE 41, a limiting rotation, d, was specified for Method 1. The value of the parameter d was set to 0.1 radians because it was thought that this rotation is large enough that it will almost never be a controlling factor in the design. For rotations greater than 0.1 radians, a more sophisticated analysis, accounting for significant geometric nonlinearity may be preferred.

NONRECTANGULAR FOOTINGS

Frequently in construction, especially in retrofit situations, a bay between columns is infilled with a shear wall, which forms "I" footprints of relatively large size. As this is a common situation, it was determined to be important to produce a reasonable set of modeling parameters and acceptance criteria for I-shaped footings. At corners, L-shaped footings are also sometimes created; but as they lack symmetry and behave quite differently, L-shapes are not considered in the component action tables.

At the time of approval of the standard, data was not available to experimentally determine the parameters g, f, and d for non-rectangular footings. It was reasoned, however, that smaller rotations are required to mobilize the capacity for I-shaped footings, just as it would require smaller curvatures to mobilize the capacity of I-shaped structural sections than of

rectangular sections of similar area. It was determined that the "missing area ratio" $MAR = (A_{rectangle} - A)/A_{rectangle}$ was a reasonable indicator of the anticipated effect of footing shape on the rotation required to mobilize the moment capacity. The component action table (Table 1) lists smaller rotations (smaller g values) required to mobilize the moment capacity for high missing area ratios. More recently, Hakhamaneshi (2014) has produced experimental data to evaluate the modeling parameters for I-shaped footings.

METHOD 1 NONLINEAR ACCEPTANCE CRITERIA

Some mechanisms involved with rocking, illustrated in Figure 8, involve gapping under the footing and limited bearing failure along the loaded edge. The critical performance measure that influences the acceptance criteria is assumed to be the residual settlement (or uplift) of the footing associated with rocking. The acceptance criteria in Table 2 are meant to ensure that the residual settlement is negligible in the case of IO and less than 1% of the footing length in the case of LS and CP performance levels.

In addition to residual settlement, another expression of damage to the foundation would be the loss of stiffness. After producing a curved soil surface through rocking action, the flat footing may come to rest with a bearing area in the center of the footing and gaps around the edges. The rotational stiffness of the footing will be deteriorated simply due to the fact that the bearing area is reduced. IO acceptance criteria are intended to avoid significant stiffness deterioration, but for the LS and CP performance levels, although there will be negligible capacity deterioration, some stiffness deterioration is expected.

MECHANISM OF RESIDUAL SETTLEMENT

The primary mechanism for the development of residual settlement is the local bearing failure under the loaded edge of the footing and the rounding of the soil-footing interface as bearing pressures are cyclically mobilized under a moving contact area. As one edge is loaded, the bearing area becomes smaller and smaller until the moment on the footing reaches

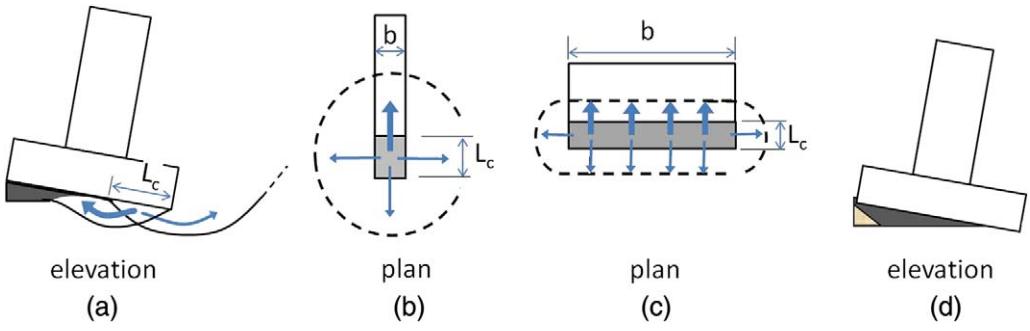

Figure 8. Mechanisms of settlement and uplift associated with rocking. (a) Localized bearing failure showing failed soil flowing back under the footing (heavy arrows) and soil flowing out from under the footing (light arrows). (b) and (c) Plan views of footing with $b \sim L_c$ and $b \gg L_c$. In (b) and (c), the shaded area represents the critical contact area, and the dashed line indicates the zone of influence of the bearing failure. (d) A potential wedge of soil that may flow under the footing to cause uplift.

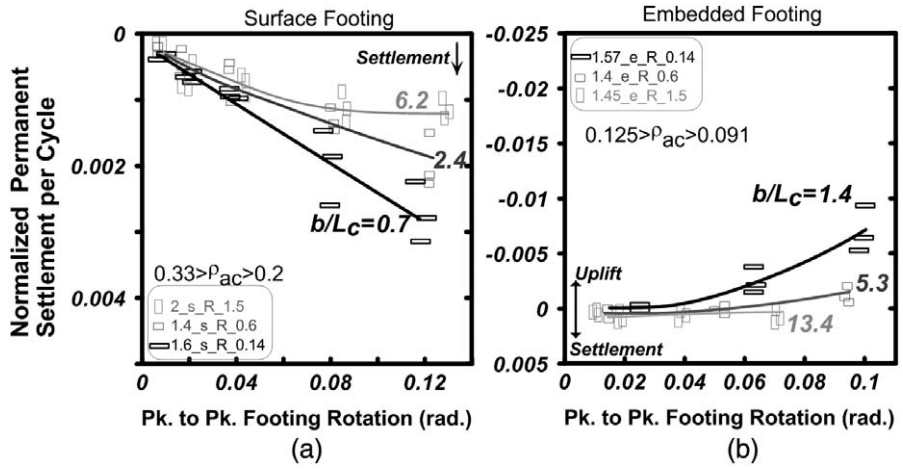

Figure 9. Normalized residual settlement per cycle of rotation for rectangular footings in dry sand. (a) Surface footings with $\rho_{ac} \approx 0.25$ to 0.35. (b) Embedded footings with $\rho_{ac} \approx 0.1$ (Hakhamaneshi et al. 2014).

its capacity corresponding to the development of a localized bearing failure on the critical contact area, as illustrated in Figure 8a. At this state, if the footing is subject to additional rotation demand, the magnitude of settlement at the outer edge of the critical contact area increases as the footing rotates about the inner edge of the critical contact area. Once this occurs the surface of the soil under the footing is no longer flat. So, as the footing rocks back in the other direction, this irregular surface is smoothed to a shape of a convex curve and some cyclically increasing settlement occurs at the center of the footing.

The magnitude of settlement is expected to depend on b/L_c. As indicated in Figure 8a, some of the soil that fails due to bearing will be pushed outward away from the footing (light arrow), contributing to settlement while some of the failing soil will be pushed back under the footing into the gap (heavy arrow), reducing the magnitude of the settlement of the center of the footing. Figure 8b and 8c show that the proportion of soil flowing back under the footing (number of heavy arrows) increases as b/L_c increases.

Figure 9 shows experimentally that the observed accumulation of settlement for rectangular footings is quite sensitive to the ratio b/L_c. Hence the acceptance criteria (allowable rotation) is significantly restricted for small values of b/L_c. Note that in Figure 9, the data points are indicated by the actual footing shapes.

MECHANISM OF RESIDUAL UPLIFT

If an embedded footing undergoes uplift associated with rocking, there is a possibility that, as a gap opens under the unloaded edge of the footing, soil will fall into or be scraped into the gap and contribute to residual uplift as illustrated in Figure 8d. The magnitude of uplift has been shown to increase with the amplitude of footing rotation by Deng and Kutter (2012) and Hakhamaneshi et al. (2012). While the uplift in their experiments may have been exaggerated by the predominant use of dry sand backfill in laboratory tests, some

experiments with moisture in the sand and some with cohesive backfill also produced residual uplift. Figure 9b shows that, as expected, the magnitude of uplift of footings is consistently correlated with the parameter b/L_c. Acceptance criteria (e.g., allowable rotations for nonlinear procedures) in ASCE 41 were set to be stricter for narrow footings and narrow flanges (footings with small values of b/L_c) and more liberal for footings with large b/L_c. Instead of showing settlement per cycle (as in Figure 9), Figure 10 shows normalized cumulative settlement as a function of cumulative rotation from many centrifuge model tests reported by Hakhamaneshi et al. (2013). The cumulative rotation is obtained by a summing up the absolute value of the peak rotations for cycles of greater amplitude than a threshold rotation ($\theta^t = 0.001$ radians). The cumulative rotation was calculated by:

$$\theta_{cum} = \sum_{i=1}^{N} |\theta_i^{rock}|, \quad \text{where } |\theta_i^{rock} - \theta_{i-1}^{rock}| \geq 2 \cdot \theta^t \tag{2}$$

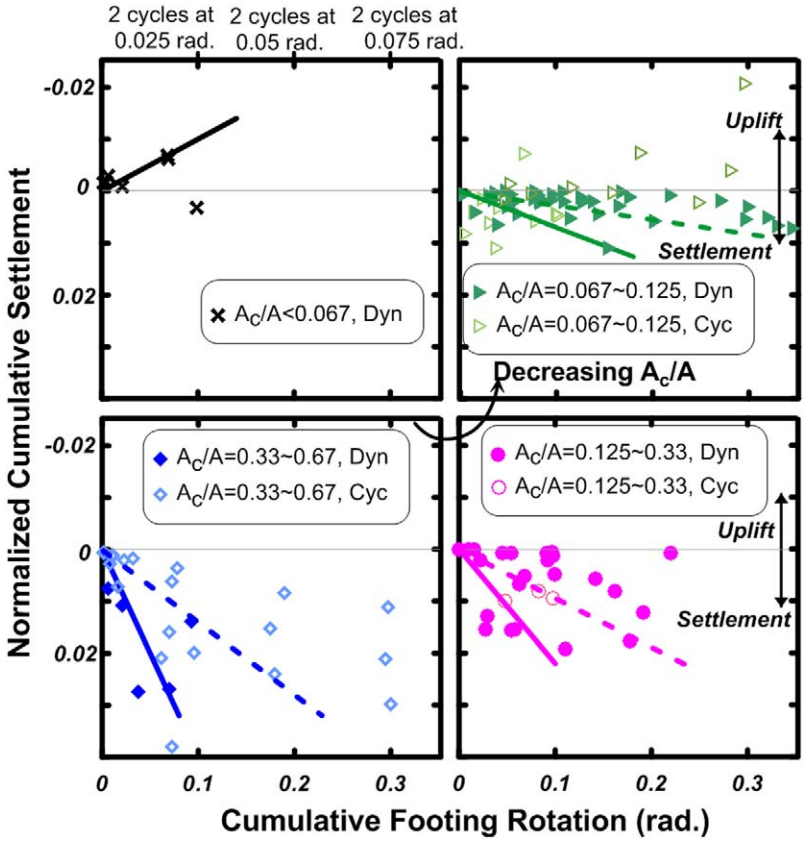

Figure 10. Normalized cumulative settlement as a function of cumulative footing rotation for different ranges of ρ_{ac} (Hakhamaneshi et al. 2012, 2013; Deng and Kutter 2012). Dashed lines represent median relations and solid lines are the envelopes proposed by Deng et al. (2014).

The main observation from all the data presented in Figure 10 is that normalized settlements (s/L) are always less than 0.01 and almost always less than 0.005 as long as the value of A/A_c is greater than 8 ($\rho_{ac} < 0.13$). There was only one exception with uplift of magnitude $s/L = 0.02$ at a cumulative rotation of 0.3 radians. This point corresponds to a narrow rectangular footing of $b/L = 0.14$ on dry sand. Excessive raveling would not be expected in natural soils that most likely will have some cohesion due to moisture or to the presence of desiccated fines.

COLLAPSE PREVENTION ACCEPTANCE CRITERIA

Figure 11 graphically plots the allowable footing rotation defined in ASCE 41 for selected rectangular and I-shaped footings as a function of $\rho_{ac} = A_c/A$. The CP acceptance criteria are based on two concepts: (1) that allowable maximum rotations should not cause excessive settlement or uplift, and (2) the limits are arbitrarily capped at large numbers beyond which it is presumed that deformations in other components of the building system will control. Specifically, footing rotations beyond 10% are never considered acceptable, even if the rocking footing would perform well beyond this value. It is very likely that a 10% rotation of a footing would cause large transient displacements that would be unacceptable to other parts of the structure (e.g., underground utility connections that pass near the

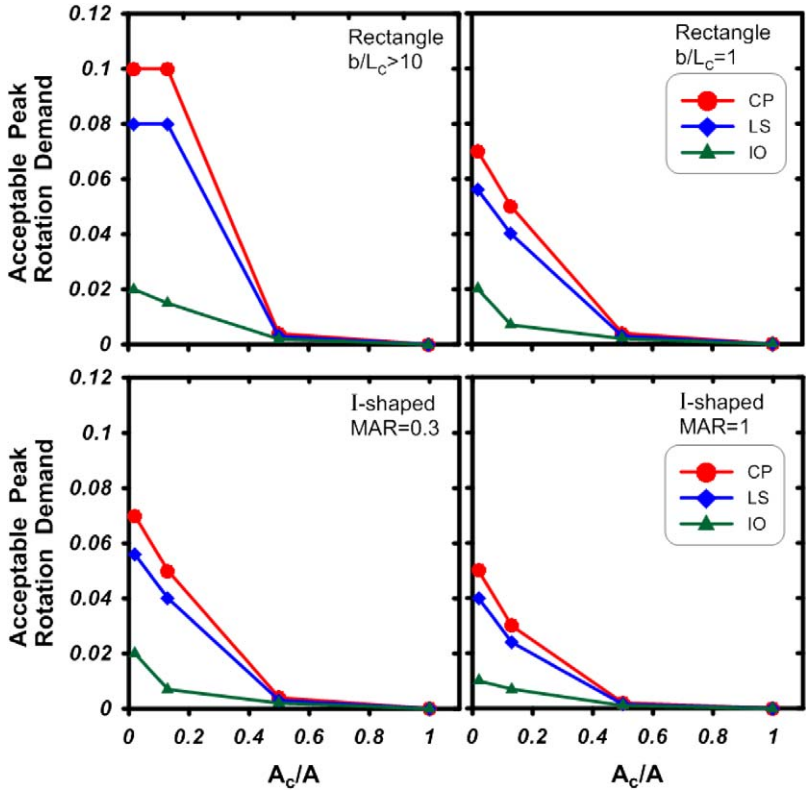

Figure 11. Acceptance criteria for peak rotation demand on rocking foundations.

footing or connections of beams or partitions to the column or shear walls that would also rotate with the footing. Hence it would usually be meaningless to accept footing rotations greater than 10%. Similarly, for IO, rotations of the footing greater than 2% are not considered acceptable even if the footing itself would not be expected to suffer significant permanent deformations. With 2% rotation of any component of a building, it is anticipated that the structure would be carefully analyzed prior to occupancy, even if footings are not expected to suffer significant permanent deformations. For LS, the acceptance criteria has been set at about 75% of that for collapse prevention.

Since settlements less than 1% of the footing length would not cause a serious concern with respect to collapse for a footing that is designed to rock, and the normalized settlement s/L is always less than 1% for footings with $\rho_{ac} < 0.13$, there is no real practical limit on the amount of footing rotation that would be acceptable for CP of a rectangular footing with $b/L_c > 10$, and rotations up to 6% are allowed for $b/L_c > 3$. In other words, permanent settlement of a rocking footing is not expected to be the cause of building collapse as long as the value of ρ_{ac} is less than 0.13.

Also apparent from Figure 11 is that relatively large settlements have been observed for rotation of footings with $\rho_{ac} > 0.5$. A 1% footing settlement could be caused by cumulative rotations of only 3% (i.e., two complete cycles of amplitude of 0.0075). Therefore, the allowable rotations were set to be very small (0.001 to 0.002) for this ρ_{ac} range. This is essentially requiring rotation to remain in the elastic range for $A_c/A = 0.5$. For $A_c/A = 1$, the footing is loaded to its bearing capacity and is on the verge of failure under vertical loads alone. Hence, the component action table does not permit such a footing to be considered as a rocking system and the allowable seismic rotation is zero.

From the definition that $b = t_f$ for I-shaped footings $t_f <$ B, and the first column of Table 1, it is apparent that the flange thickness, t_f must be greater than the critical contact length L_c. If this condition was not met, the footing would become unstable as the entire flange thickness is required to support the vertical load and no additional resistance is available to resist rotation of the footing, especially in the case of a small or non-existent web thickness for the I-shape.

The allowable rotations for $MAR = 0.3$ are similar to those for a rectangular footing with $b/L_c = 1$. An I-shaped footing with the theoretical limiting case of 100% missing area ratio (a non-existent footing) has allowable rotations that are listed at about 30% of the allowable rotations for a rectangle with $b/L_c > 10$. The reason for reducing the allowable rotations for I-shapes is that the anticipated residual settlements and uplifts are expected to be greater for I-shapes than for rectangular shapes; there is a greater perimeter of the footing along which material may escape or fall in under the footing by the mechanisms described earlier for rectangular footings.

METHOD 1: LINEAR PROCEDURES

For linear analysis procedures (LSP or LDP) in ASCE 41, the designer has the choice of assuming a fixed base (neglecting foundation flexibility) or a flexible base. For fixed base analysis, the *m*-factor for foundation soil is defined as 1.5 for IO, 3.0 for LS, and 4.0 for CP.

For flexible base models, the *m*-factors are obtained from Table 8-3 in ASCE-41 and are dependent on footing parameters. Excerpts of this table are given in Table 3.

DETERMINATION OF *m*-FACTORS

The *m*-factor acceptance criteria may be thought of as the maximum allowable moment (or force) demand in a linear analysis divided by the elastic yield strength. Although the *m*-factor is defined to be the ratio of moments (or forces), if one assumes validity of the "equal displacement rule," the *m*-factor is equal to the ratio of allowable to yield rotation or $m = \theta_{allowable}/\theta_y$. The allowable rotation may be taken directly from Table 1, and the yield rotation could be calculated by Equation 3, using a suitable expression for rocking stiffness, K_θ.

Table 3. Excerpts from Table 8-3 of ASCE 41-13: Modeling parameters and numerical acceptance criteria for linear procedures

			m-Factors[1]		
			Performance Level		
Footing Shape			IO	LS	CP
(a) Rectangle[2]					
b/L_c	$(A_{rect} - A)/A_{rect}$	A_c/A			
≥10	0	0.02	3	7	10
		0.13	2	6	9
		0.5	1	1	1
		1	1	1	1
3	0	0.02	3	7	10
		0.13	2	5	8
		0.5	1	1	1
		1	1	1	1
(b) I-shape[2]					
$1 \le b/L_c \le 10$	0.3	0.02	3	7	10
		0.13	1	3	5
		0.5	1	1	1
		1	–	–	–
$1 \le b/L_c \le 10$	0.6	0.02	3	7	10
		0.13	1.5	3	5
		0.5	1	1	1
		1	–	–	–

[1] Linear interpolation between values listed in the table shall be permitted.
[2] Where a foundation is subject to uplift, the *m*-factor shall be applied to the restoring dead load.

$$\theta_y = \frac{M_c}{K_\theta} \tag{3}$$

The rocking moment capacity of the footing, M_c, may be calculated from Equation 1 for rectangular footings.

NEW EMPIRICAL ROTATIONAL STIFFNESS EQUATION

Initially the idea was to use equations already defined in ASCE 41, which are based upon elasticity theory, to determine the rotational stiffness (e.g., stiffness K_{yy} in Equation 4a with embedment correction factor β_{yy} in Equation 4b):

$$\textit{Rocking about y-axis} \qquad K_{yy\text{-}surf} = \frac{GB^3}{1-\nu}\left[0.47\left(\frac{L}{B}\right)^{2.4} + 0.034\right] \tag{4a}$$

$$\textit{Rocking about y-axis} \qquad \beta_{yy} = 1 + 1.4\left(\frac{d}{L}\right)^{0.6}\left[1.5 + 3.7\left(\frac{d}{L}\right)^{1.9}\left(\frac{d}{D}\right)^{-0.6}\right] \tag{4b}$$

The predictions using this approach are compared to initial stiffness for the trilinear model fit to the experimental data by Johnson (2012) in Figure 12a. The quality of the fit is reasonable, but is not especially pleasing. Equations 4a and 4b are somewhat difficult to evaluate, especially considering uncertainty in elastic properties, and the fact that some nonlinearity may

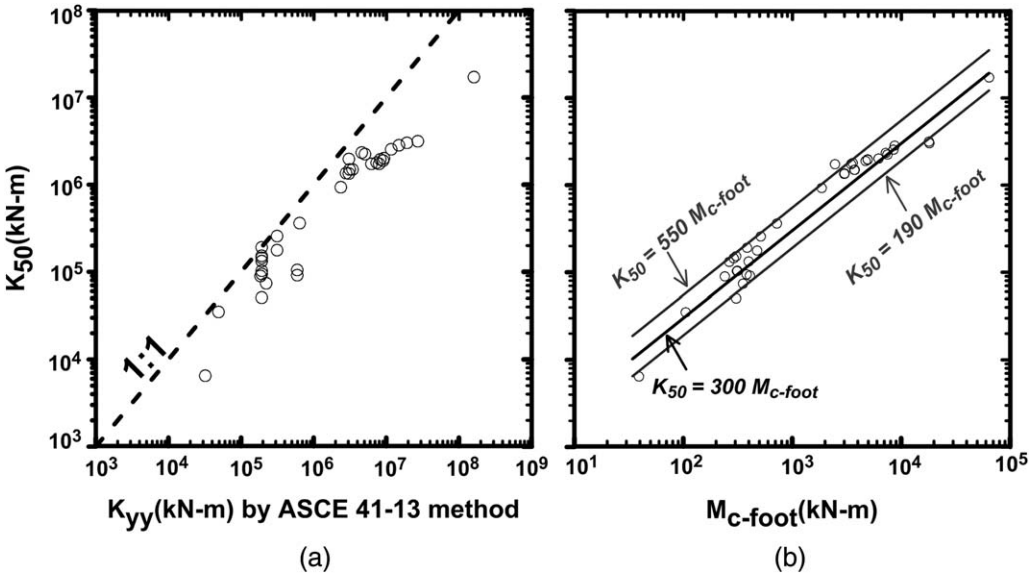

Figure 12. (a) Comparison between stiffness computed using FEMA (2000) equations (e.g., Equation 4a) and K_{50} obtained by fitting experimental data to the trilinear model. (b) Correlation between moment capacity of a rocking footing and K_{50} (Deng et al. 2014, Hakhamaneshi et al. 2016).

develop even if the moment is only on the order of a third of the moment capacity. Therefore, an empirical correlation between the rotational stiffness (the initial segment for a trilinear model) and the moment capacity is considered, as reported by Deng et al. (2014):

$$K_{50} = (172 \; to \; 460) \cdot M_c \tag{5}$$

Since the adoption of the new ASCE 41 standard, Hakhamaneshi et al. (2014) obtained additional data and supported this approach, but gave a range of 190 to 550 instead of 172 to 460 in Equation 5. The larger values (up to 550) are associated with I-shaped footings. The correlation between moment capacity computed from Equation 1 and the experimentally measured initial stiffness from the trilinear model is presented in Figure 12b. Despite its simplicity, the empirical equation seems to perform well compared to the theoretical elasticity-based equations. As a value of 300 is a reasonable average of 172 and 460, a simplified version of Equation 5, namely, $K_{50} = 300\,M_c$, was adopted for determination of *m*-factors. Interestingly, based on the empirical procedure, the yield rotation (the rotation that would be required to mobilize the moment capacity at the initial stiffness) is the reciprocal of the coefficient in Equation 5. If the average value of 300 is adopted as a coefficient, we get simply $\theta_y \approx M_c/K_{50} = 1/300$. Going one step further, the *m*-factor consistent with the nonlinear acceptance criteria and the equal displacement rule is $m_{edr} = \theta_{allowable}/\theta_y$ which was calculated by dividing the allowable rotation from Table 1 by the rotation to cause yield (1/300). The *m*-values in Table 3 (Table 8-3 of ASCE 41), were set to approximately equal the calculated m_{edr} except the *m*-values were capped at 10, rounded down using engineering judgment, and *m*-factors less than 1 were not used.

The values in the published Table 8-3 for $MAR = 0.3$ and 1.0 do not consistently follow the intended trend of that m should decrease as *MAR* increases. The effect of this in the table is relatively minimal, but should be updated in the next to capture the intended trend.

METHOD 2: BEAM ON GAPPING SPRINGS

Method 2 uses nonlinear gapping foundations springs that account for the coupling between axial load and moment capacity. The coupling between vertical load and moment arises due to the dependence of rocking moment capacity on vertical load. Method 2 also explicitly calculates gapping associated with uplift and this effect can directly be accounted for in a numerical simulation. However, in Method 2, the horizontal shear forces do not affect the vertical bearing capacity or moment capacity of the footing, although it is well known that the shear forces will increase the critical contact area, and hence, will affect the moment capacity of the footing (Gajan et al. 2010). Thus Method 2, like Method 1, is best suited for rocking-dominated footings.

MODELING PROCEDURES

Method 2 usually assumes that the structural footing is relatively rigid and that the flexibility of the system is derived from spring deflection (elastic and nonlinear) and/or gapping in the soil springs below the footing-soil interface. This method may also be performed using macroelement-type formulations (e.g., Gajan et al. 2010, Figini et al. 2012, Chatzigogos et al. 2009), many of which are able to capture the coupling between the bearing, sliding, and rotational deformation mechanisms. Due to their complexity, these models tend to have

to be implemented in custom software and may not be readily available to the design professional. If not available, the moment-rotation and vertical load-settlement behavior may be modeled using a series of vertical nonlinear gapping springs (beam on nonlinear Winkler foundation or BNWF model). An example of this model is depicted in Figure 2b.

Gajan et al. (2010) compare the performance of a BNWF model and a macroelement model and provide guidance in selection of the nonlinear properties of the BNWF spring model. ASCE 41-13 uses a similar approach for determining the elastic properties of the springs as was used in ASCE 41-06. Stiffer springs are used along the rocking edges of the footing in order to allow approximate matching of the moment stiffness (rotation about the y-axis) and vertical stiffness (translation in the z-direction) from elasticity equations presented in ASCE 41-13. The bearing capacity of BNWF springs may be obtained by setting the spring capacity per unit area equal to the expected bearing capacity on the critical contact area. The tension capacity of the springs is set to zero and a no-tension gap is to be modeled. If the spacing of the springs is greater than the critical contact length, L_c, then one spring could unrealistically take the entire vertical load without yielding. The spacing of the springs should be small enough to ensure that yielding of the springs under the bearing loads can occur at the loaded edge of the footing. This may be accomplished by limiting the spacing of the springs to be less than $L_c/2$. The BNWF model can also directly capture the approximate permanent settlements. In ASCE 41-13, the allowable rotations for a foundation modeled using Method 2 are the same as those for Method 1 (see the IO, LS, and CP limits in Table 1).

METHOD 3: BEAM ON GAPPING SPRINGS WITH NON-RIGID FOOTING

Non-rigid footings include foundations for which the deformation of the structural footings must be accounted for either because the structural footing yields plastically (e.g., a plastic hinge forms in the footing structural slab) or deforms elastically (e.g., where the footing thickness is small compared to the footing area). The soil-footing interaction is modeled by compression-only sub-grade springs with uniform stiffness based upon elastic solutions for beams and plates in contact with elastic foundations. The footing rotation caused by soil deformation is subject to the same acceptance criteria as for Method 1 (see Tables 2 and 3). However, the satisfactory performance of the structural footing with respect to yielding and deformation should be separately evaluated with the appropriate acceptance criteria.

OTHER CHANGES RELEVANT TO ROCKING SHALLOW FOOTINGS

Updated relations for determining the shear modulus in ASCE 41 include correlations between SPT blow count and shear modulus, use of shear wave velocity data to determine shear modulus and a method to account for the effect of the footing pressure on the confining pressure and hence shear modulus. In addition, explicit guidance is included in the standard regarding the location below the footing at which the shear modulus, G, should be determined. The consideration of uncertainty in soil properties on the rotational capacity and stiffness was also changed. As in the previous version of ASCE 41, the strength and capacity of the foundation for vertical or horizontal translation should be multiplied and divided by $(1 + C_v)$ where C_v is the coefficient of variation. Without additional information about the value of C_v at a particular site, C_v may be taken as 1. However, it is important to note that the moment capacity has less uncertainty than the shear and axial capacity.

For moment capacity, the uncertainty is evaluated using Equation 1 with upper and lower bound values of the vertical load, and by varying the value of q_c by a factor of $(1 + C_v)$.

BUILDING RETROFIT DESIGN EXAMPLE

An actual building retrofit project was used as the basis for an example analysis using linear procedures to evaluate a rocking shallow foundation. The analysis is reported in some detail in the online Appendix and compares results for previous versions of ASCE 31 and ASCE 41 to the new provisions. For the example, a new reinforced concrete shear wall is added between two existing concrete columns supported on spread footings that are tied together with a grade beam to form a 33 ft-long, 8 ft-wide I-shaped footing with a missing area ratio of $MAR = 39\%$. The prescriptive expected bearing capacity, q_c, for a spread footing is calculated using the equation found in the ASCE 41 standard and is equal to $q_c = 3 \cdot q_{allow} = 12\,\text{ksf}$.

Using the LSP in ASCE 31-03 and a force reduction R-factor ($R_{OT} = 8$ for LS), the footing was found to be *adequate*.

Using the LSP in ASCE 41-06 with a fixed base assumption, the foundation soil is classified as deformation-controlled, acceptance criteria for foundation soil is based on an m-factor $= 3$, and the use of the upper-bound capacity ($2q_c$) is permitted; the footing was found to be *inadequate* using this methodology.

Using the LSP in ASCE 41-06 with a flexible base assumption, the strength of the soil would not need to be evaluated; effectively allowing infinite ductility of the rocking system and the foundation would hence be considered to be *adequate*.

Lastly, using ASCE 41-13, an evaluation was assumed to be performed using a flexible base LDP for which the moment demand was reduced by 25% below that used for the ASCE 31-03 or 41-06 analyses listed above. The m-factor from Table 8-3 of ASCE 41-13 produced $m = 2.4$ and revealed the I-shaped footing to be *inadequate* by a large margin, even with the 25% reduced moment demand. However, by widening the footing from 8 ft to 11 ft and by filling in all of the missing area, a satisfactory rocking foundation could be obtained for this example building. It is believed that ASCE 41-13 properly accounts for the accumulation of settlement beneath rocking footings that may occur if the ρ_{ac} value is large, especially for narrow footings. The blanket use of $R_{OT} = 8$ in ASCE 31-03 or the assumption that the soil strength need not be evaluated if the footing is modeled by linear springs in ASCE 41-06 does not consider potential detrimental effects of footing settlement. Analysis of an existing footing with a slightly higher axial compression ratio $\rho_{ac} = A_c/A$ than that which is presented in the online Appendix example reveals a potential inconsistency in the current ASCE 41-13 foundation provisions. In the approximate range of $0.15 < \rho_{ac} < 0.3$, the calculated m-factor is about equal to or less than the permitted m-factor of 3 for fixed base models. In other words, there can be certain instances where it is advantageous (i.e., more liberal) for soil-foundation analysis if a less complex modeling approach is used, which is not the intent of ASCE 41. Either the fixed base m-factor could be limited to less than 3 or the m-factors in Table 8-3 for flexible base analysis with $0.15 < \rho_{ac} < 0.3$ could be increased to resolve this inconsistency.

DISCUSSION

While the new provisions in ASCE 41-13 described herein were initially intended to encourage the use of rocking foundations in practice, it has been found that the new provisions in many cases tend to restrict the use of rocking due to the low *m*-factors and small allowable rotations for $\rho_{ac} > 0.15$, especially for narrow footings. ASCE 41-13 performance criteria were intended to limit foundation settlements to be less than 1% of the footing length. Large potential settlements may develop for $A_c/A > 0.3$, as illustrated in Figure 9 and Figure 10. The acceptance criteria in ASCE 41-13 could be liberalized if larger settlements potentially could be tolerated; the tolerable settlement may be determined by the contents, stiffness and ductility of the building.

It bears repeating that the value of A_c/A is meant to be determined from expected ultimate soil capacities, not from a factor on allowable capacities. The assumption that the ultimate capacity is three times the allowable capacity may be conservative in many cases and may lead to conservative evaluation of the ability of foundations to resist rocking rotations while minimizing settlements. By the prescriptive method for building retrofit, the allowable bearing stress, q_{allow}, is obtained from old geotechnical reports and then the expected ultimate bearing capacity is assumed to be $q_c = 3 \cdot q_{allow}$. Furthermore, if the effect of the coefficient of variation is considered, with $(1 + C_v) = 2$, then the lower bound of the value of A_c/A increases by a factor of 2 and may produce even smaller *m*-factors and very small allowable rotations (see Figure 11). The capacity should not be reduced by $(1 + C_v)$ if the prescriptive approach used to determine bearing capacity is already conservative. More efficient designs could be obtained, and inconsistencies between ASCE 41-13 and previous versions of the code might be resolved if an in-situ measurement of soil shear strength was used in place of the prescriptive method for determining soil capacities.

CONCLUSIONS

This paper describes the logic behind the changes to ASCE 41-13 with respect to evaluation and design of rocking shallow foundations as part of assessing or retrofitting existing buildings. The new acceptance criteria are largely based on controlling residual settlements associated with rocking. In experiments in the field and on the centrifuge, the residual settlements are always small if the compression ratio value of $\rho_{ac} = A_c/A < 0.13$. Hence, the new standard allows large demands for footings with small ρ_{ac}. As footing settlement is sensitive to footing shape, the allowable rotation depends on footing shape which is quantified by the ratio of b/L_c and Missing Area Ratio. The goal of the tabulated acceptance criteria is to limit footing settlements associated with rocking to be less than 1% of the footing length. If larger settlements could be tolerated, more efficient designs may be obtained by directly evaluating settlements using a more rigorous procedure.

The standard permits the evaluation and design of rocking foundations through three different methods. Method 1 is for use of uncoupled springs in each direction; hence,the interaction between shear, axial and moment loads are neglected. Method 2, involving sub-grade reaction springs with no-tension gapping, accounts for coupling between axial load and moment capacity. Hence, Method 2 is preferred if axial loads are expected to vary during seismic loading. Method 3 applies to cases where the deformation of the structural footing is significant. An example is presented in the online Appendix to illustrate the

application of the new standard to an example based upon a real building retrofit project and compared the design with that obtained from previous versions of the standard.

An inconsistency in the new standard was identified for linear procedures wherein smaller m-values can be obtained for a dynamic flexible base analysis than for fixed base analysis. This runs counter to the intent of ASCE 41 that more sophisticated analysis should not be penalized by more severe acceptance criteria.

There would be substantial benefit to more accurately quantifying the bearing capacity of soil in-situ. The soil bearing capacity has little effect on the moment capacity of a footing, but has substantial effect on the acceptance criteria, especially if A_c/A is close to 0.5. The new provisions in the component action tables for linear and nonlinear procedures are only applicable to rocking-dominated footings, i.e., footings with large normalized moment to shear ratio ($M/VL > 1$). Consideration of additional data from footings with smaller moment to shear ratios (e.g., Hakhamaneshi 2014) is needed to extend the tables to sliding footings or footings with coupled rocking and sliding deformations.

ACKNOWLEDGMENTS

The work presented in this paper was the product of many years of work, collaborations with many individuals, funding from many agencies including PEER, Caltrans, and NSF, most recently through NSF award CMMI-0936503. Any findings, statements and conclusions are those of the authors, and do not reflect the opinions of the sponsoring organizations. The authors would like to especially thank the suggestions and contributions of Prof. Sashi Kunnath, Prof. Tara C. Hutchinson, Prof. Lijun Deng, Prof. Mark Aschheim, Kenneth Johnson, Dr. Weian Liu, and Andreas Gavras for substantial contributions and discussions related to this paper.

APPENDIX

Please refer to the online version of this paper to access the supplementary example.

REFERENCES

American Society of Civil Engineers (ASCE), 2003. *Seismic Evaluation of Existing Buildings* (ASCE/SEI 31-03), 2003, Reston, VA.

American Society of Civil Engineers (ASCE), 2007. *Seismic Rehabilitation of Existing Buildings* (ASCE/SEI 41-06), 2007, Reston, VA.

American Society of Civil Engineers (ASCE), 2014. *Seismic Evaluation and Retrofit of Existing Buildings* (ASCE/SEI 41-13), 2014, Reston, VA.

Chatzigogos, C. T., Pecker, A., and Salencon, J., 2009. Macroelement modeling of shallow foundations, *Soil Dynamic and Earthquake Engineering* **29**, 765–781.

Deng, L., and Kutter, B. L., 2012. Characterization of rocking shallow foundations using centrifuge model tests, *Earthquake Engng. Struct. Dyn.* **41**, 1043–1060.

Deng, L., Kutter, B., and Kunnath, S., 2014. Seismic design of rocking shallow foundations: displacement-based methodology, *J. Bridge Eng.*, 10.1061/(ASCE)BE.1943-5592.0000616.

Figini, R., Paolucci, R., and Chatzigogos, C. T., 2012. A macro-element model for non–linear soil–shallow foundation–structure interaction under seismic loads: theoretical development and experimental validation on large scale tests, *Earthquake Engineering & Structural Dynamics* **41**, 475–493.

Gajan, S., and Kutter, B. L., 2009. Effect of moment-to-shear ratio on combined cyclic load-displacement behavior of shallow foundations from centrifuge experiments, *J. Geotech. Geoenviron. Engrg.*, DOI: 10.1061/(ASCE)GT.1943-5606.0000034.

Gajan, S., Raychowdhury, P., Hutchinson, T. C., Kutter, B. L., and Stewart, J. P., 2010. Application and validation of practical tools for nonlinear soil-foundation interaction analysis, *Earthquake Spectra* **26**, 111–129.

Hakhamaneshi, M., Kutter, B. L., Deng, L., Hutchinson, T. C., and Liu, W., 2012. New findings from centrifuge modeling of rocking shallow foundations in clayey ground, *Proceedings of ASCE 2012 Geo-Congress*, 25–29 March 2012, Oakland, CA.

Hakhamaneshi, M., Kutter, B. L., Hutchinson, T. C., and Liu, W., 2013. Rocking Foundations on Clayey Environment-MAH01, Network for Earthquake Engineering Simulation, Data set, DOI:10.4231/D3GT5FF2T.

Hakhamaneshi, M., 2014. Rocking Foundations for Building Systems, Effect of Footing Shape, Soil Environment, Embedment and Normalized Moment-to-Shear Ratio, Ph.D. Thesis, University of California, Davis, CA.

Hakhamaneshi, M., Kutter, B. L., Moore, M., and Champion, C., 2016. Validation of ASCE 41-13 modeling parameters and acceptance criteria for rocking shallow foundations, *Earthquake Spectra* **32**, 1121–1140.

Johnson, K. E., 2012. Characterization of Test Results of Rocking Shallow Foundations Using a Multi-Linear Hysteretic Model, M.S. Report, University of California, Davis, CA.

National Institute of Standards and Technology (NIST), 2012. Soil-Structure Interaction For Building Structures, Report # NIST GCR 12-917-21, prepared by NEHRP Consultants Joint Venture, for National Institute of Standards and Technology, Gaithersburg, MD.

Negro, P., Paolucci, R., Pedretti, S., and Faccioli, E., 2000. Large-scale soil-structure interaction experiments on sand under cyclic loading, in *Proc., 12th World Conf. on Earthquake Engineering*.

Poland, C. E., 2008. ASCE 41-06: Seismic rehabilitation of existing buildings: A new tool for achieving seismic safety, *Structure Magazine*, National Council of Structural Engineers Associations.

Rosebrook, K. R., and Kutter, B. L., 2011a. *Soil-Foundation-Structure Interaction: Shallow Foundations*, Centrifuge Data Rep. for test series KRR01, Rep. No. UCD/CGMDR-01/09, University of California, Davis, CA.

Rosebrook, K. R., and Kutter, B. L., 2001b. *Soil-Foundation-Structure Interaction: Shallow Foundations*, Centrifuge Data Rep. for test series KRR02, Rep. No. UCD/CGMDR-01/10, University of California, Davis, CA.

(Received 19 December 2014; accepted 27 July 2015)